Norm-conserving and ultrasoft pseudopotentials for first-row and transition elements

1994 J. Phys.: Condens. Matter 6 8245

(http://iopscience.iop.org/0953-8984/6/40/015)

J. Phys.: Condens. Matter 6 (1994) 8245–8257. Printed in the UK

Norm-conserving and ultrasoft pseudopotentials for first-row and transition elements

G Kresse and J Hafner

Institut für Theoretische Physik, Technische Universiät Wien, Wiedner Hauptstraße 8–10, A-1040 Wien, Austria

Received 18 April 1994

Abstract. The construction of accurate pseudopotentials with good convergence properties for the first-row and transition elements is discussed. We show that by combining an improved description of the pseudowavefunction inside the cut-off radius with the concept of ultrasoft pseudopotentials introduced by Vanderbilt optimal compromise between transferability and plane-wave convergence can be achieved. With the new pseudopotentials, basis sets with no more than 75–100 plane waves per atom are sufficient to reproduce the results obtained with the most accurate norm-conserving pseudopotentials.

1. Introduction

The theoretical study of the properties of materials via electronic-structure calculations is currently an extremely active field of research. Much of the recent progress in this area is due to the success of the local-density approximation (LDA) to the density-functional theory of many-electron systems [1, 2]. One of the most efficient techniques for performing self-consistent electronic-structure and total-energy calculations within the LDA is based on the pseudopotential description of the electron–ion interaction and the use of plane-wave basis sets [3, 4]. In particular, the development of the Car–Parrinello molecular-dynamics technique [5], the use of efficient conjugate-gradient techniques for the variational determination of the ground state [6, 7], or the use of methods for iterative diagonalization of large matrices [8, 9, 10] allows for the investigation of systems with a large number of inequivalent atomic sites in the unit cell. However, the use of these techniques is still difficult for materials such as the first-row elements (B, C, N, O, ...) and the 3d transition metals because a large number of plane waves is necessary to describe the 'localized' 2p, respectively 3d, valence states of these materials. Therefore many attempts [11, 12, 13] have been made to generate smooth pseudopotentials optimized for the convergence of the plane-wave expansion of the total energy. Quite generally it was found that the cut-off energy for the plane-wave expansion (i.e. the highest kinetic energy of a plane wave) may be reduced by increasing the cut-off radius R_c where the pseudowavefunction is matched to the all-electron wavefunction. Increasing R_c however reduces the accuracy and transferability, and the difficulty consists in matching these two conflicting requirements.

Several strategies for optimization of pseudopotentials have been proposed. It is now generally agreed that it is most convenient to construct the pseudowavefunctions directly. For a continuous pseudopotential, the pseudowavefunctions must be continuously differentiable at least twice at the cut-off radius R_c, i.e.,

$$\phi_{l\epsilon}^{\mathrm{PS}}(r)^{(n)}\Big|_{r=R_c} = \phi_{l\epsilon}^{\mathrm{AE}}(r)^{(n)}\Big|_{r=R_c} \qquad n = 0, 1, 2, \ldots \tag{1}$$

0953-8984/94/408245+13$19.50

where $\phi_{l\epsilon}^{AE}(r)$ is the solution of the radial Schrödinger equation for a specific energy ϵ

$$\left[\frac{\hbar^2}{2m}\left(-\frac{d^2}{dr^2}+\frac{l(l+1)}{r^2}\right)+V(r)-\epsilon\right]\phi_{l\epsilon}^{AE}(r)=0 \tag{2}$$

and $\phi_{lm\epsilon}^{AE}(r) = Y_{lm}(r)\phi_{l\epsilon}^{AE}(r)/r$. Second, the charge enclosed within the cut-off radius R_c must be the same for the pseudowavefunctions and all-electron wavefunction (norm-conservation constraint)

$$\int_0^{R_c}\phi_{l\epsilon}^{ps}(r)^2\,dr=\int_0^{R_c}\phi_{l\epsilon}^{AE}(r)^2\,dr. \tag{3}$$

An *ansatz* for the pseudowavefunction $\phi_{l\epsilon}^{ps}(r)$ must have a minimum of four adjustable parameters in order to satisfy conditions (1) and (3). Additional parameters [11, 12] are introduced with the aim of improving the convergence of an expansion of the pseudowavefunctions in a basis of plane waves. The pseudopotential can be obtained by an inversion of the radial Schrödinger equation. The non-local factorized Kleinman–Bylander (KB) pseudopotential operator [14] is simply given by

$$V = V_{loc}+\sum_{lm}\frac{|\chi_{lm\epsilon}\rangle\langle\chi_{lm\epsilon}|}{\langle\chi_{lm\epsilon}|\phi_{lm\epsilon}^{ps}\rangle} \tag{4}$$

with

$$|\chi_{lm\epsilon}\rangle = -(T+V_{loc}-\epsilon)|\phi_{lm\epsilon}^{ps}\rangle \tag{5}$$

where V_{loc} is a local potential which is—in principle—arbitrary. In practice, the local part of the pseudopotential is of considerable importance. A reasonable choice avoids the appearance of so called 'ghost states' beneath the reference energies ϵ (the existence of 'ghost states' is thoroughly discussed in [15]) and helps to reduce the strength [15]

$$E_l^{strength}=\frac{\langle\chi_{l\epsilon}|\chi_{l\epsilon}\rangle}{\langle\chi_{l\epsilon}|\phi_{l\epsilon}^{ps}\rangle} \tag{6}$$

of the non-local part of the pseudopotential.

An entirely new pseudopotential concept has recently been proposed by Vanderbilt [16]. This new concept is characterized by two main points. (i) More than one reference energy ϵ per quantum state l is allowed. This guarantees an excellent transferability over a wide energy range even for larger cut-off radii R_c. Similar ideas have been developed by Blöchl [17]. If a generalized norm-conservation condition is satisfied, the new pseudopotential operators are Hermitian (see below). (ii) Dropping the norm-conservation constraint leads to a new class of pseudopotentials, for which a generalized eigenvalue problem has to be solved. Because the norm-conservation constraint does not apply, a charge-density deficit between the pseudowavefunctions and exact wavefunctions exists. This deficit is described by localized augmentation functions. A close connection between these augmentation charges and the overlap operator in the generalized eigenvalue problem exists.

Vanderbilt's scheme allows us to construct 'ultrasoft' pseudopotentials requiring not more than 50–100 plane waves per atom, even for the difficult cases of the 2p and 3d elements. In the present paper we first present a revised Rappe, Rabe, Kaxiras, and Joannopoulos (RRKJ) scheme, which can be used to construct rather soft norm-conserving pseudopotentials. In section 4 we discuss the extension of this scheme to ultrasoft Vanderbilt pseudopotentials, and demonstrate the success of our scheme for some difficult elements.

2. Optimized norm-conserving pseudopotentials

As we mentioned in section 1, the direct construction of a pseudowavefunction is a convenient way to construct a pseudopotential. In agreement with RRKJ, we think that spherical Bessel functions form the most natural basis set to expand the pseudowavefunctions $\phi_{l\epsilon}^{PS}(r)$ within the cut-off radius:

$$\phi_{l\epsilon}^{PS}(r) = \sum_{i=1}^{n} \alpha_i r j_l(q_i r) \tag{7}$$

with q_i chosen such that

$$\frac{\partial}{\partial r}\left(\ln \phi_{l\epsilon}^{AE}(r)\right)\Big|_{r=R_c} = \frac{\partial}{\partial r}\left(\ln(r j_l(q_i r))\right)\Big|_{r=R_c} \tag{8}$$

and that there are $(i-1)$ zeros within $r < R_c$. This basis set has the distinct advantage of being orthogonal and (for $n \to \infty$) complete. Due to the fitting of the logarithmic derivative of the spherical Bessel functions one needs a minimum of only three terms to satisfy the requirements of norm conservation (3) and continuity of the first two derivatives of the pseudowavefunction at R_c (1). RRKJ proposed to add a variable number of terms (up to $n = 10$) and to exploit the additional parameters to minimize the kinetic energy contained in the Fourier components of ϕ^{PS} beyond a certain cut-off Q_{cut} (with $E_{cut} = (\hbar^2/2m)Q_{cut}^2$), i.e.

$$\Delta E_{kin}(Q_{cut}) = \frac{\hbar^2}{2m}\int_{Q_{cut}}^{\infty} \tilde{\phi}_{l\epsilon}^{PS}(q)^2 q^2 \, dq \Rightarrow \text{Min} \tag{9}$$

where $\tilde{\phi}_{l\epsilon}^{PS}(q)$ is defined as

$$\tilde{\phi}^{PS}(q) = \sqrt{\frac{2}{\pi}}\int_0^{\infty} \phi^{PS}(r) j_l(qr) qr \, dr. \tag{10}$$

In practice it turns out that it is more convenient to define a convergence limit ΔE for the kinetic energy and to determine Q_{cut} such that $\Delta E_{kin}(Q_{cut}) < \Delta E$. The resulting pseudopotential is optimized for a basis set containing all plane waves with $G < Q_{cut}$. RRKJ proposed to use a large set of spherical Bessel functions (up to $n = 10$). However, it turns out that this leads to an oscillatory behaviour of the pseudopotential in real space without really reducing $\Delta E_{kin}(Q_{cut})$. Therefore Lin and co-workers [18] proposed to use only $n = 4$, i.e. the minimum number of Bessel functions that allows for the minimization of the kinetic energy. In this case Q_{cut} is chosen as $Q_{cut} = q_4$ since it is effectively controlled by the highest wavenumber of the Bessel functions. In practice we find that the optimization of the kinetic energy is unnecessary and that $n = 3$ leads to a smooth pseudowavefunction with excellent convergence properties. Only for very small cut-off radii (R_c smaller than the position of the first maximum of the all-electron wavefunction) was a fourth term in the expansion (7) sometimes necessary to guarantee a nodeless pseudoorbital. However we found that such small cut-offs were not necessary to construct high-quality pseudopotentials.

The restriction to only three Bessel functions also makes the generation of pseudopotentials for unbound states unproblematic. As it stands the kinetic-energy criterion applies only to bound states which can be expanded in a sum of Bessel functions. It is in principle possible to rewrite the kinetic-energy criterion for a finite interval $[0, R_{check}]$. However we found that this generalization is numerically cumbersome, and does not allow for a reasonable optimization of pseudowavefunctions. Without optimization the construction of pseudopotentials for unbound states is straightforward. This is important in many cases, e.g. for the construction of d pseudopotentials for B-group elements (no bound

d state exists for atomic configurations). In this paper we use the atomic configuration of the free atom (s^2p^2 for C and Ge, s^2p^4 for O, and $d^{10}s^1$ for Cu) as the reference configuration for the calculation of the pseudopotential. The kinetic-energy criterion is not only useful for optimizing the pseudowavefunction, but also helps to estimate the necessary energy cut-off for a total-energy calculation. Therefore we calculate the necessary cut-offs Q_{cut} for a set of energy errors $\Delta E = 10$ mRyd, ..., 0.1 mRyd as a routine task for any pseudopotential. This can be done in a numerically stable way by transforming the wavefunctions $\phi^{ps}(r)$ to their reciprocal-space representation $\tilde{\phi}^{ps}(q)$ using for instance fast Fourier transformations. In general the errors ΔT of the kinetic energy evaluated in reciprocal space

$$\Delta T = \frac{\hbar^2}{2m}\int_0^\infty \phi^{ps}(r)\Big(-\frac{d^2}{dr^2}+\frac{l(l+1)}{r^2}\Big)\phi^{ps}(r)\,dr - \frac{\hbar^2}{2m}\int_0^\infty \tilde{\phi}^{ps}(q)^2 q^2\,dq \tag{11}$$

are smaller than 10^{-5} Ryd.

In figure 1 we show the validity of the kinetic-energy criterion. The markers show the convergence of a total-energy plane-wave calculation using a cut-off of E_{cut} for (a) diamond and (b) face-centred-cubic copper for different pseudopotentials. The lines represent the errors expected from the kinetic-energy criterion using the atomic pseudowavefunctions. A similar agreement was found for all elements considered up to now. In general the cut-off $E_{cut} = (\hbar^2/2m)Q_{cut}^2$ should be large enough to reduce the kinetic-energy error ΔE_{kin} to 1 mRyd; for very accurate calculations the cut-off E_{cut} might be chosen so that the error is smaller that 0.1 mRyd.

Table 1. Comparison of the accuracy and convergence properties of various types of s-electron pseudopotential for Ge. The first column lists the cut-off radius R_c necessary to achieve a comparable accuracy (measured in terms of the logarithmic derivatives of the wavefunction, calculated at $R = 2.4$ au and energies ± 0.5 Ryd below and above the reference energy, columns two and three). The fourth and fifth columns list the cut-off energies E_{cut} necessary to converge the kinetic energy to within $\Delta E_{kin} < 1$ mRyd (0.1 mRyd). See text.

				E_{cut} (Ryd)	
Potential	R_c (au)	$\Delta E(-0.5)$ (Ryd)	$\Delta E(0.5)$ (Ryd)	1 mRyd	0.1 mRyd
BHS	1.25	−0.0030	−0.000 57	23	32
VAN	1.3	−0.0026	−0.000 55	16	31
TM	2.25	−0.0034	−0.000 65	24	41
RRKJ3	2.5	−0.0023	−0.000 47	15	18
RRKJ4	2.2	−0.0026	−0.000 48	15	29
RRKJ6	2.0	−0.0029	−0.000 54	15	91

Tables 1–3 compare the accuracy and transferability of different types of pseudopotential: Bachelet, Hamann, and Schlüter (BHS [19]), Vanderbilt (VAN [20]), Troullier–Martins (TM [12]) potentials and RRKJ potentials with $n = 3, 4, 6$ were considered. $n = 3$ corresponds to no optimization of the kinetic energy, optimization for $n = 4, 6$ was done for an error $\Delta E = 1$ mRyd (for $n = 4$ this criterion is almost equivalent to the criterion of Lin *et al* [18]). Accuracy and transferability are measured in terms of the errors in the logarithmic derivative at an energy 0.5 Ryd above and below the reference energy (for copper 0.2 Ryd because the d band is relatively narrow). The convergence is characterized by the cut-off energies E_{cut} necessary to converge the kinetic energy of the atomic pseudowavefunction up to an error of 1 mRyd, respectively 0.1 mRyd (i.e. $\Delta E_{kin}(Q_{cut}) < 1$ (0.1) mRyd). As characteristic examples we chose the s pseudopotential

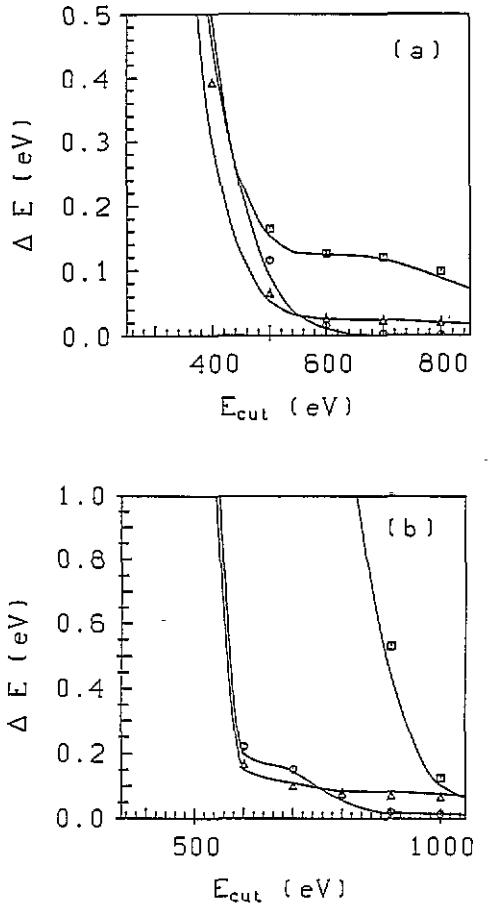

Figure 1. Illustration of the kinetic-energy-convergence criterion: convergence of a total-energy plane-wave calculation using norm-conserving pseudopotentials (a) for diamond and (b) for face-centred-cubic copper. Squares are results for BHS pseudopotentials ((a) R_c = 0.85 au, (b) R_c = 1.05 au), circles for the RRKJ3 pseudopotential ((a) R_c = 1.6 au, (b) R_c = 2.0 au), triangles for the RRKJ6 pseudopotential ((a) R_c = 1.4 au, (b) R_c = 1.9 au). The full lines represent the errors expected from the kinetic-energy criterion evaluated using *atomic* pseudowavefunctions (errors for one s electron and three p electrons were taken into account for diamond, for copper errors corresponding to ten d electrons were calculated). The energy differences ΔE are calculated relative to the total energy obtained with E_{cut} = 3000 eV.

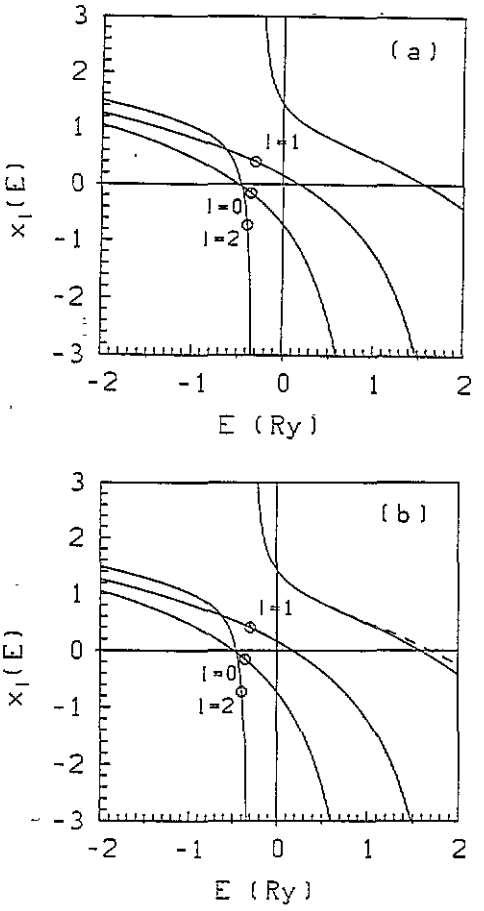

Figure 2. Logarithmic derivatives $x_l(E)$ for Cu at R = 2.7 au. Full lines, calculated for the all-electron potential; dashed lines, (a) calculated for norm-conserving Vanderbilt pseudopotential with two reference energies for d states, (b) calculated for the US pseudopotential (see text for description of pseudopotentials).

of Ge (a 'classical pseudopotential element'), the p pseudopotential of C, and the d pseudopotential of Cu (two examples for the difficult cases of the first-row and transition elements). In all cases we find the following.

Table 2. Same as table 1, but for p-electron pseudopotential in C. Logarithmic derivatives are calculated at $R = 1.9$ au.

				E_{cut} (Ryd)	
Potential	R_c (au)	$\Delta E(-0.5)$ (Ryd)	$\Delta E(0.5)$ (Ryd)	1 mRyd	0.1 mRyd
BHS	0.85	0.0024	0.0040	70	89
VAN	1.0	0.0020	0.0040	50	65
TM	1.7	0.0025	0.0041	40	67
RRKJ3	1.6	0.0024	0.0040	40	48
RRKJ4	1.5	0.0024	0.0041	39	70
RRKJ6	1.4	0.0024	0.0041	38	202

Table 3. Same as table 1, but for d-electron pseudopotential in Cu. Errors in the logarithmic derivatives are calculated at $R = 2.8$ au and ± 0.2 Ryd from the reference energy.

				E_{cut} (Ryd)	
Potential	R_c (au)	$\Delta E(-0.2)$ (Ryd)	$\Delta E(0.2)$ (Ryd)	1 mRyd	0.1 mRyd
BHS	1.05	0.0157	0.0296	73	106
VAN	1.3	0.0165	0.0304	80	97
TM	2.3	0.0153	0.0284	61	102
RRKJ3	2.0	0.0157	0.0297	54	80
RRKJ4	1.95	0.0148	0.0282	46	90
RRKJ6	1.9	0.0152	0.0287	45	155

(i) The BHS and VAN pseudopotentials require very small cut-off radii in order to ensure transferability (small $\Delta E(\pm 0.5)$), and this leads to relatively large cut-off energies.

(ii) The TM pseudopotential allows the largest cut-off radii, but the improvement of convergence is modest. Only for C does the TM pseudopotential reach the same quality as the RRKJ3 pseudopotential.

(iii) In conjunction with the RRKJ pseudopotentials it is also possible to use relatively large cut-off radii. The largest cut-off radii are allowed within the RRKJ3 scheme. Inclusion of more than the minimum number of Bessel functions requires a smaller R_c.

We would like to point out again that the RRKJ4 and RRKJ6 pseudopotentials were optimized for $\Delta E_{kin}(Q_{cut}) < 1$ mRyd. But even for this accuracy the necessary energy cut-offs are only a few Ryd smaller than without optimization. For any accuracy other than 1 mRyd the necessary energy cut-offs are larger than for the RRKJ3 scheme (in tables 1–3 this is only demonstrated for 0.1 mRyd, but this also holds for 10 mRyd).

The disappointing performance of the TM and RRKJ4, 6 schemes has a common origin: the additional degrees of freedom lead to a $\phi^{PS}(r)$ that deviates very rapidly from the all-electron wavefunction $\phi^{AE}(r)$ for $r < R_c$. For the TM scheme the problem is slightly reduced due to the requirement of continuous higher derivatives at R_c. The kinetic-energy optimization simply transfers kinetic energy to Q-components smaller than Q_{cut}, but at the same time reduces the transferability. In addition, the optimization creates a pseudopotential which converges slowly beyond Q_{cut} (see the long tail of ΔE for the RRKJ6 pseudopotentials in figure 1).

Therefore in all cases the RRKJ scheme with the minimum number of parameters works best. However, at comparable transferability, the cut-off energies required for the C p and

Cu 3d pseudopotentials are larger than those required for Ge s potentials by a factor of three (C) to four (Cu).

3. Inclusion of more than one reference energy

Vanderbilt (and independently Blöchl) [16, 17] proposed to use a second reference energy in the construction of the factorized pseudopotential. This can be done in the following way. For each quantum number l and each reference energy ϵ one constructs a pseudowavefunction ϕ^{ps} satisfying (1) and (3). For each pseudowavefunction one defines a function χ_i as in equation (5)

$$|\chi_i\rangle = -(T + V_{\mathrm{loc}} - \epsilon)|\phi_i^{\mathrm{ps}}\rangle \tag{12}$$

where i is a shorthand notation for quantum numbers l, m and the reference energy ϵ, $i = (lm, \epsilon)$. It is now possible to define a basis β_i which is dual to ϕ_i^{ps},

$$\langle\beta_i|\phi_j^{\mathrm{ps}}\rangle = \delta_{ij} \tag{13}$$

via

$$|\beta_i\rangle = \sum_j (B^{-1})_{ij}|\chi_j\rangle \tag{14}$$

and

$$B_{ij} = \langle\phi_j^{\mathrm{ps}}|\chi_i\rangle. \tag{15}$$

The non-local factorized pseudopotential operator can be written as

$$V^{\mathrm{NL}} = \sum_i |\chi_i\rangle\langle\beta_i| = \sum_{i,j} B_{ij}|\beta_j\rangle\langle\beta_i|. \tag{16}$$

It may be shown that B_{ij} and therefore the pseudopotential V^{NL} are Hermitian if the pseudowavefunctions ϕ_i^{ps} fulfill a generalized norm-conservation constraint

$$Q_{ij} = \langle\phi_j^{\mathrm{AE}}|\phi_i^{\mathrm{AE}}\rangle - \langle\phi_j^{\mathrm{ps}}|\phi_i^{\mathrm{ps}}\rangle = 0 \tag{17}$$

or explicitly (assuming spherical symmetry)

$$Q_{l\epsilon,l\epsilon'} = \int_0^{R_c} \left(\phi_{l\epsilon}^{\mathrm{AE}}(r)\phi_{l\epsilon'}^{\mathrm{AE}}(r) - \phi_{l\epsilon}^{\mathrm{ps}}(r)\phi_{l\epsilon'}^{\mathrm{ps}}(r)\right) \mathrm{d}r = 0. \tag{18}$$

This step considerably improves transferability and allows for increased cut-off radii without compromising accuracy. Although the step is simple and the necessary changes in a total-energy program are negligible, only a few authors [21, 22] tried to work out norm-conserving Vanderbilt pseudopotentials. The reason is that the additional constraint

$$Q_{l\epsilon,l\epsilon'} = 0 \tag{19}$$

for $\epsilon \neq \epsilon'$ might be cumbersome to implement. Therefore Chou [21] constructed a Hermitian approximation to the Vanderbilt pseudopotentials, in which the generalized norm-conservation condition need not apply. Using this approximation it is possible to construct the pseudowavefunctions for all reference energies independently requiring only $Q_{l\epsilon,l\epsilon} = 0$. Morrison and co-workers [22] showed that Chou's algorithm was hard to implement for Ag; nevertheless they were able to construct an exact norm-conserving Vanderbilt pseudopotential for Ag. In our work we generally also neglect the additional constraint (19). The weaker condition $Q_{l\epsilon,l\epsilon} = 0$ leads to a non-Hermitian B_{ij}, but in conjunction

with our new minimal-pseudopotential-generation scheme (RRKJ3) the differences in $B_{ij}-B_{ji}$ are generally small, i.e. if we simply use the Hermitian matrix

$$\bar{B}_{ij} = \frac{B_{ij} + B_{ji}}{2} \tag{20}$$

instead of B_{ij}, the logarithmic derivatives are accurate over a wide energy range. For Cu and C the second reference energy reduces the error in the logarithmic derivatives almost to zero. Figure 2(a) illustrates this for Cu. We created a scalar-relativistic pseudopotential for the atomic configuration $3d^{10}4s^1$. For the s and p components the cut-off was set to $R_c = 2.7$ au. For the d pseudopotential two reference energies (one 50 mRyd above the bound state) and a radial cut-off of $R_c = 2.0$ au were used. We chose the s component as the local part of the pseudopotential operator. The radial cut-off of $r_e = 2.7$ au seems to be relatively large (especially if we consider the bond length of the dimer $R_b = 4.2$ au), but as shown in figure 3 the logarithmic derivatives are still exact at $R = 2.0$ au, i.e. well inside the cut-off radius. This once again demonstrates that the RRKJ3 pseudopotential reproduces the scattering properties of the all-electron potential rather accurately even at small distances.

Figure 4(a) shows the logarithmic derivatives for C. The pseudopotential was created for the atomic configuration $2s^21p^2$. In this case we used two reference energies for the s and the p states and one for the d component (second reference energy for s and p wavefunctions 50 mRyd above the bound state). Cut-off radii for all pseudowavefunctions are $R_c = 1.2$ au. As local potential we used the d pseudopotential.

4. Ultrasoft Vanderbilt pseudopotentials

The second step of the Vanderbilt scheme consists in relaxing the norm-conservation constraint (18,19). The 'ultrasoft' (US) pseudowavefunctions ϕ_i^{us} must satisfy only equation (1). *Therefore the pseudopotential operator is no longer Hermitian; but it is possible to* transform the standard eigenvalue problem

$$(T + V_{loc} + V^{NL} - \epsilon)|\phi\rangle = 0 \tag{21}$$

to a generalized eigenvalue problem

$$(T + V_{loc} + \bar{V}^{NL} - \epsilon S)|\phi\rangle = 0 \tag{22}$$

with a Hermitian overlap operator

$$S = 1 + \sum_{i,j} Q_{ij}|\beta_j\rangle\langle\beta_i| \tag{23}$$

and a Hermitian pseudopotential operator

$$\bar{V}^{NL} = \sum_{i,j} D_{ij}|\beta_j\rangle\langle\beta_i| \tag{24}$$

where

$$D_{ij} = B_{ij} + \epsilon_i Q_{ij}. \tag{25}$$

It can be shown that the logarithmic derivative is not only correct at each reference energy ϵ_i but also for small variations around each reference energy ϵ_i. The transition to the generalized eigenvalue problem also changes the electron density involved in a self-consistent calculation [23]

$$n(r) = \sum_n f_n|\phi_n(r)|^2 + \sum_{n,ij} f_n\langle\phi_n|\beta_j\rangle\langle\beta_i|\phi_n\rangle Q_{ij}(r) \tag{26}$$

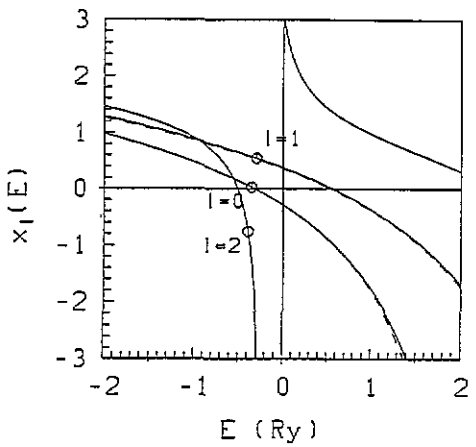

Figure 3. Logarithmic derivatives $x_l(E)$ for Cu at $R = 2.0$ au. Full lines, calculated for the all-electron potential; dashed lines, calculated for norm-conserving Vanderbilt pseudopotentials (see text for description of pseudopotentials).

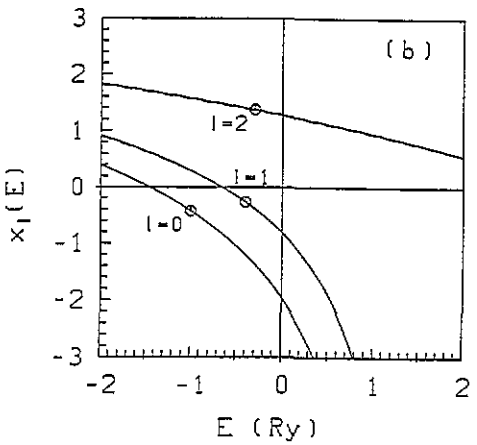

Figure 4. Logarithmic derivatives $x_l(E)$ for C at $R = 1.6$ au. Full lines, calculated for the all-electron potential; dashed lines, (a) calculated for norm-conserving Vanderbilt pseudopotential with two reference energies for s and p states, (b) calculated for the US pseudopotential (see text for description of pseudopotentials).

where the augmentation functions $Q_{ij}(r)$ are defined as

$$Q_{ij}(r) = \phi_i^{\mathrm{AE}}(r)\phi_j^{\mathrm{AE}}(r)^* - \phi_i^{\mathrm{US}}(r)\phi_j^{\mathrm{US}}(r)^*. \tag{27}$$

In order to calculate the augmentation part of the charge density (second term in equation (26)) efficiently, it is convenient to replace the $Q_{ij}(r)$ by appropriate pseudized functions $Q_{ij}^{\mathrm{PS}}(r)$. We do this by replacing the all-electron wavefunctions ϕ_i^{AE} in equation (27) by their norm-conserving counterparts ϕ_i^{PS} (a different scheme was proposed in [16, 23]). The ultrasoft pseudopotential constructed this way possesses almost the same properties as the norm-conserving pseudopotential.

Figure 2(b) shows the logarithmic derivatives for a US Cu pseudopotential. In comparison to figure 2(a) only the d component was changed. For the ultrasoft d pseudopotential we used a cut-off of $R_{\mathrm{c,d}} = 2.7$ au for both reference energies; the

augmentation functions were calculated using the norm-conserving pseudowavefunctions for $R_{aug} = 2.0$ au.

Figure 4(b) demonstrates the quality of the US pseudopotential for C. We used a cut-off radius of $R_c = 1.8$ au for all components; the augmentation functions were calculated using the norm-conserving pseudowavefunctions for $R_{aug} = 1.2$ au. As local potential we chose a norm-conserving d pseudopotential with $R_c = 1.8$ au. As can be seen from figures 2(b) and 4(b) the quality of the logarithmic derivatives is excellent for both US potentials. However, there is a second source of errors which cannot be assessed this way. The problem arises if the potential is transferred to a different chemical environment. In the Vanderbilt scheme this error is mainly controlled by the quality of the augmentation functions (in our case by the quality of the norm-conserving pseudowavefunctions from which the augmentation functions are constructed). In order to check the accuracy of our pseudopotentials we calculated the equilibrium properties of crystalline phases. For copper we also performed a calculation for the dimer, using a simple cubic supercell of 10 Å.

The calculations for the crystal and the supercell containing the dimer have been performed using the VASP (Vienna *ab initio* simulation program) [8, 24] code which performs a variational solution of the Kohn–Sham equations using conjugate-gradient techniques. To describe the wavefunctions, a small energy cut-off E_{cut} is necessary. The action of the local potential on the wavefunction and the smooth part of the charge density (first term in equation (26)) can be calculated using a relatively coarse fast-Fourier-transform (FFT) grid which must contain all wavevectors up to $G = 2G_{cut}$. Non-locality is handled in the real-space projection scheme [25]. A finer grid is necessary to represent the augmentation charges (second term in equation (26)) and for the calculation of the Hartree and exchange–correlation potential. All operations involving $Q_{ij}(r)$ are performed on this second grid in real space. The total time spent on the fine grid scales linearly with the number of ions and is negligible compared with the computational costs necessary for one conjugate-gradient step on the wavefunctions. One of the consequences of the introduction of ultrasoft pseudopotentials is that the gradients of the free energy with respect to the orbitals ϕ_n are now given by

$$|g_n\rangle = (H - \epsilon_n S)|\phi_n\rangle \tag{28}$$

(note that (28) holds only if the Hamiltonian is diagonal in the subspace spanned by ϕ_n). The gradient defined this way is no longer orthogonal to the orbitals ϕ_n i.e. $\langle\phi_{n'}|S|g_n\rangle \neq 0$. We resolve this problem by preconditioning the the search vector and explicitly orthogonalizing the vector after preconditioning

$$|g_n^c\rangle = \Big(1 - \sum_{n'} |\phi_{n'}\rangle\langle\phi_{n'}|S\Big)K|g_n\rangle. \tag{29}$$

In our work we use the preconditioning functions K of [6]. The preconditioned gradient g_n^c is used in conjunction with a sequential band-by-band optimization of the the expectation value of the Hamiltonian $\langle\phi_n|H|\phi_n\rangle/\langle\phi_n|\phi_n\rangle$ [9]. After running over all bands (including some empty bands), a subspace diagonalization is performed, the Fermi energy and new partial occupancies are calculated, and the charge density $n(r)$ and the potential $V(r)$ are updated. We found that the convergence speed does not suffer by the introduction of the overlap operator; in general the the number of steps required to calculate the ground state is the same as for norm-conserving pseudopotentials.

Tables 4 and 5 show results for different Cu pseudopotentials. For FCC Cu we used a mesh of $4 \times 4 \times 4$ Monkhorst–Pack [26] k-points in the irreducible wedge of the FCC Brillouin zone. This mesh is not sufficient to get accurate structural energy differences, but

Table 4. Lattice constant a_0, equilibrium volume V_0, bulk modulus B_0 and cohesive energy E_c (relative to non-spin-polarized atom) for face-centred-cubic Cu, and bonding length r_e, cohesive energy D_e, and vibrational frequency ω_e for a Cu_2 dimer using pseudopotentials which differ in the description of the d component. $R_{c,d}$ is the cut-off for the norm-conserving, respectively ultrasoft, d wavefunctions and E_{cut} the cut-off energies necessary to converge the kinetic energy of the atomic pseudowavefunction to within $\Delta E_{kin} < 1$ mRyd.

	NC[a]	US[b]	US[b]	US[b]
$R_{c,d}$ (au)	2.0	2.0	2.3	2.7
E_{cut} (Ryd)	50	25	18	14
V_0 (Å^3)	11.11	11.11	11.11	11.11
a_0 (Å)	3.542	3.542	3.542	3.542
B_0 (Mbar)	1.80	1.80	1.79	1.78
E_c (eV)	−4.69	−4.68	−4.68	−4.67
r_e (Å)		2.17	2.175	2.185
D_e (eV)		3.19	3.19	3.19
ω_e (cm^{-1})		308	303	314

[a] Norm-conserving pseudopotential using two d reference energies as described in section 3.
[b] Ultrasoft pseudopotential; augmentation functions were calculated from the norm-conserving pseudowavefunctions for $R_{aug} = 2.0$ au.

Table 5. Same as table 4 for ultrasoft pseudopotentials ($R_{c,d} = 2.7$ au, $E_{cut} = 12$ Ryd) varying the precision of the augmentation functions (i.e. using different cut-offs R_{aug} for the norm-conserving d wavefunctions); in addition results for an accurate *non-factorized* pseudopotential are shown (NC, $R_{c,d} = 1.1$ au).

	R_{aug} (au)			
	2.0	1.6	1.2	NC
V_0 (Å^3)	11.11	11.13	11.19	11.21
a_0 (Å)	3.542	3.544	3.550	3.552
B_0 (Mbar)	1.78	1.72	1.69	1.70
E_c (eV)	−4.67	−4.62	−4.58	−4.61
r_e (Å)	2.185	2.18	2.185	
D_e (eV)	3.19	3.19	3.17	
ω_e (cm^{-1})	314	306	315	

it is good enough to compare different pseudopotentials. In table 4 we varied the cut-off for the US d pseudowavefunctions. As can be seen the results remain almost unchanged a radial cut-off of up to $R_{c,d} = 2.7$ au—leading to a cut-off energy of only 14 Ryd—is definitely possible. As a second check we changed the precision of the augmentation functions (table 5): using a very accurate augmentation function ($R_{aug} = 1.2$ au) changes the cohesive energy by approximately 0.1 eV and the equilibrium volume by 1%, which is a small but still reasonable error. Using different pseudopotential cut-off radii $R_{c,d}$ in conjunction with a varying R_{aug} leads to the same result. Table 5 shows in addition the results obtained with a non-factorized norm-conserving RRKJ3 pseudopotential with a very small cut-off radius (leading to a cut-off energy $E_{cut} \simeq 2000$ eV). Because of the high accuracy of the pseudopotential and the very large basis set, and because errors that could be introduced by Kleinman–Bylander factorization are avoided, this is the most accurate (but expansive) calculation that can be done within this framework.

The results for the dimer show a similar trend: the precision of the augmentation functions is less important in the dimer, mainly because the environment does not change very much on going from the atom to the dimer. Once again the changes with the cut-off for the US d pseudowavefunctions are very small.

Table 6. Lattice constant a_0, equilibrium volume V_0, bulk modulus B_0 and cohesive energy E_c (relative to the spin-polarized atom) for diamond for different pseudopotentials. R_c is the cut-off for the pseudowavefunctions, E_{cut} the cut-off energies necessary to converge the kinetic energy of the atomic pseudowavefunction to within $\Delta E_{kin} < 1$ mRyd.

	NC[a]	US[b]	US[b]	US[b]
R_c (au)	1.2	1.4	1.6	1.8
E_{cut} (Ryd)	60	33	25	20
V_0 (Å^3)	5.49	5.49	5.49	5.50
a_0 (Å)	3.527	3.527	3.529	3.530
B_0 (Mbar)	4.60	4.60	4.61	4.61
E_c (eV)	−9.03	−9.03	−9.03	−9.01

[a] Norm-conserving pseudopotential using two s and p reference energies and one d reference energy (see also section 3).

[b] Ultrasoft pseudopotential; augmentation functions were calculated using the norm-conserving pseudowavefunctions for $R_{aug} = 1.2$ au; d pseudopotential is norm conserving and used as the local potential.

Table 7. *Same as table 6 for ultrasoft pseudopotentials ($R_c = 1.4$ au) varying the precision* of the augmentation functions (i.e. using different cut-offs R_{aug} for the norm-conserving wavefunctions).

	R_{aug} (au)		
	1.0	1.2	1.4
V_0 (Å^3)	5.50	5.49	5.46
a_0 (Å)	3.530	3.527	3.525
B_0 (Mbar)	4.60	4.60	4.59
E_c (eV)	−9.024	−9.03	−9.04

Tables 6 and 7 show results for different C pseudopotentials for diamond. The calculations were done using a $4 \times 4 \times 4$ k-point grid in the irreducible wedge of the Brillouin zone. All pseudopotentials give very similar results: a cut-off of $R_{aug} = 1.2$ au for the augmentation functions and a pseudopotential cut-off radius of $R_c = 1.8$ au are sufficient to produce an accurate C pseudopotential; the cut-off energy is only 20 Ryd. A more extensive test for the C pseudopotentials will be published elsewhere [27].

5. Conclusion

We have reconsidered the construction of efficient and accurate pseudopotentials for the first-row and transition elements. We show that for norm-conserving pseudopotentials an optimal compromise between transferability and plane-wave convergence can be achieved within a modified RRKJ scheme. The introduction of two reference energies allows us to improve the transferability of the norm-conserving potentials. A substantial reduction of the cut-off energy for the plane-wave expansion results from the introduction of ultrasoft

potentials without norm conservation (the pseudowavefunctions in the core region being described by the modified RRKJ scheme). The combination of all three features leads to accurate ultrasoft pseudopotentials for 2p and 3d elements requiring 75–100 plane waves per atom. C and Cu have been treated here as representative examples, but similar results have been obtained for the 2p elements Li, B, N, and O, for the 3d elements V, Cr, Mn, Fe, Co, and Ni, and for some 4d elements. This opens the way to *ab initio* molecular-dynamics simulations for these difficult materials. First results for liquid Cu and V have been published recently [28].

Acknowledgment

This work has been supported by Siemens–Nixdorf Austria within the contract of cooperation with the Technische Universität Wien.

References

[1] Hohenberg P and Kohn W 1964 *Phys. Rev.* **136** B864
Kohn W and Sham L 1965 *Phys. Rev.* **140** A1133
Kohn W 1985 *Highlights of Condensed Matter Theory* ed M P Tosi, M Fumi and F Bassani (Amsterdam: North-Holland)
[2] Jones R O and Gunnarsson O 1989 *Rev. Mod. Phys.* **61** 689
[3] Ihm J 1988 *Rep. Prog. Phys.* **51** 105
[4] Pickett W E 1989 *Comput. Phys. Rep.* **9** 115
[5] Car R and Parrinello M 1985 *Phys. Rev. Lett.* **55** 2471
[6] Teter M P, Payne M C and Allan D C 1989 *Phys. Rev.* B **40** 12255
[7] Payne M C, Teter M P, Allan D C, Arias T A and Joannopoulos J D 1992 *Rev. Mod. Phys.* **64** 1045
[8] Kresse G and Hafner J 1993 *Phys. Rev.* B **47** RC558; *Phys. Rev.* B **48** 13115
[9] Bylander D M, Kleinman L and Lee S 1990 *Phys. Rev.* B **42** 1394
[10] Wood D M and Zunger A 1984 *J. Phys. A: Math. Gen.* **18** 1343
[11] Rappe A M, Rabe K M, Kaxiras E and Joannopoulos J D 1990 *Phys. Rev.* B **41** 1227
[12] Troullier N and Martins J L 1991 *Phys. Rev.* B **43** 1993
[13] Kresse G, Hafner J and Needs R J 1992 *J. Phys.: Condens. Matter* **4** 7451
[14] Kleinman L and Bylander D M 1982 *Phys. Rev. Lett.* **48** 1425
[15] Gonze X, Käckell P and Scheffler M 1990 *Phys. Rev.* B **41** 12264
Gonze X, Stumpf R and Scheffler M 1991 *Phys. Rev.* B **44** 8503
[16] Vanderbilt D 1990 *Phys. Rev.* B **41** 7892
[17] Blöchl P E 1990 *Phys. Rev.* B **41** 5414
[18] Lin J S, Qteish A, Payne M C and Heine V 1993 *Phys. Rev.* B **47** 4174
[19] Bachelet G B, Hamann D R and Schlüter M 1982 *Phys. Rev.* B **26** 4199
[20] Vanderbilt D 1985 *Phys. Rev.* B **32** 8412
[21] Chou M Y 1992 *Phys. Rev.* B **45** 11465
[22] Morrison I, Bylander D M and Kleinman L 1993 *Phys. Rev.* B **47** 6728
[23] Laasonen K, Pasquarello A, Car R, Lee C and Vanderbilt D 1993 *Phys. Rev.* B **47** 10142
[24] Kresse G 1993 *Thesis* Technische Universität, Wien
[25] King-Smith R D, Payne M C and Lin J S 1991 *Phys. Rev* B **44** 13063
[26] Baldereschi A 1973 *Phys. Rev.* B **7** 5212
Monkhorst H J and Pack J D 1976 *Phys. Rev.* B **13** 5188
[27] Furthmüller J, Hafner J and Kresse G to be published
[28] Kresse G and Hafner J 1993 *Phys. Rev.* B **48** 13115